Title
DYNAMICAL AND APPROXIMATE LEED THEORIES APPLIED TO LAYERS OF LARGE MOLECULES

Authors
Hove, M.A. Van
Somorjai, G.A.

Publication Date
1981-05-01

LBL-12803
Preprint

Lawrence Berkeley Laboratory
UNIVERSITY OF CALIFORNIA

Materials & Molecular
Research Division

Submitted to Surface Science

DYNAMICAL AND APPROXIMATE LEED THEORIES APPLIED TO LAYERS OF LARGE MOLECULES

M.A. Van Hove and G.A. Somorjai

May 1981

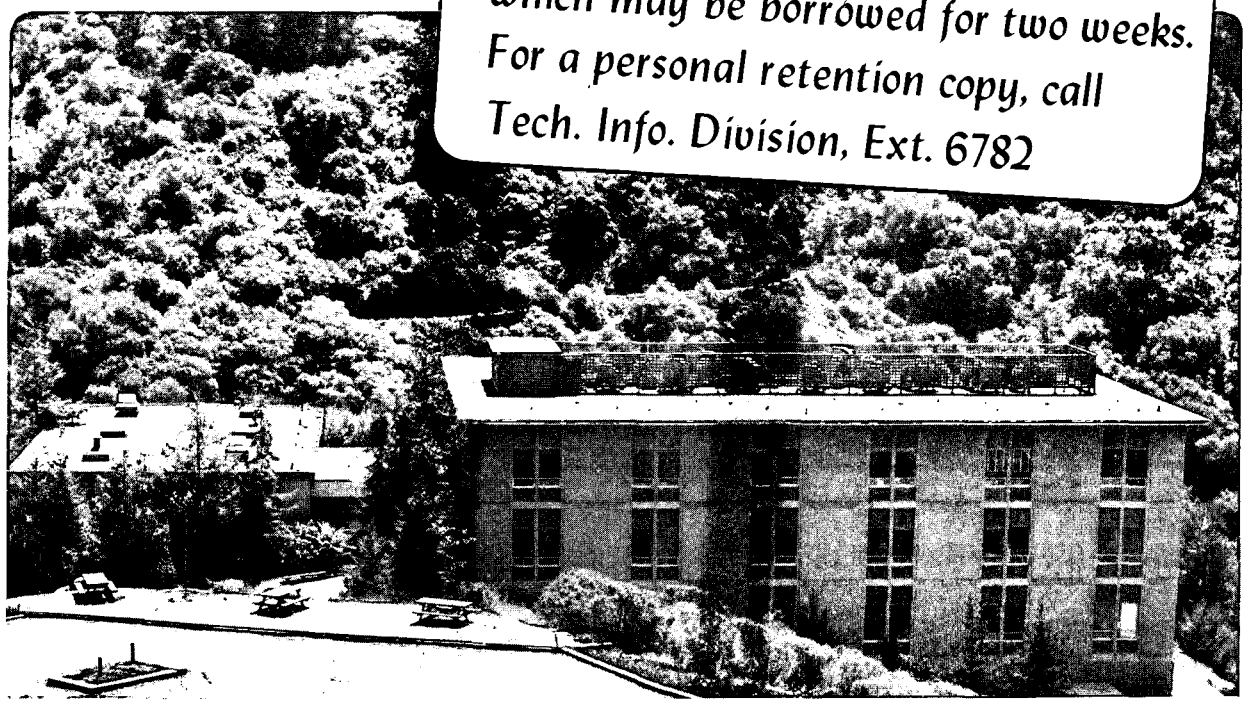

Prepared for the U.S. Department of Energy under Contract W-7405-ENG-48

DISCLAIMER

LBL 12803

DYNAMICAL AND APPROXIMATE LEED THEORIES APPLIED TO LAYERS OF LARGE MOLECULES

M.A. Van Hove and G.A. Somorjai

Materials and Molecular Research Division, Lawrence Berkeley Laboratory,
and
Department of Chemistry, University of California, Berkeley, CA 94720

Abstract

A theoretical study is carried out of the application of the Combined Space Method (CSM) in low energy electron diffraction (LEED) from large molecules, for which rings of six carbon atoms arranged in periodic layers are chosen. The marked sensitivity of calculated intensity-energy (I-V) curves to variations of the geometry of these rings is exhibited. The reduction of the computation effort through approximations characterized by various degrees of neglect of multiple scattering is explored. It is shown that efficient approximate methods can be applied in the structural determination of large molecules at surfaces, at the very least in preliminary unrefined searches through sets of plausible structures. A new class of approximations based on near-neighbor multiple scattering is proposed that has efficient features for multiple use in structural searches.

This work was supported by the Director, Office of Energy Research, Office of Basic Energy Sciences, Materials Sciences Division of the U.S. Department of Energy under contract W-7405-ENG-48.

1. Introduction

The analysis of low energy electron diffraction (LEED) intensities for the structural determination of adsorbed small molecules has now been applied to a number of relatively simple cases. These are CO, studied on Ni(100),[1a-d] Cu(100),[1a] Pd(100),[2] and Rh(111),[3] and C_2H_2 (acetylene) and C_2H_4 (ethylene) studied in two structures (metastable and stable) on Pt(111)[4] and on Rh(111).[5] For the hydrocarbons, most calculations ignored the presence of hydrogen atoms in the molecules because hydrogen is hardly detectable by LEED in these cases.[4] It appears that experiments in the near future are aiming to determine the surface structure of organic molecules of increasing size with more than two carbon atoms per molecule. It is therefore appropriate to explore the next step, that of larger molecules.

A central question in considering larger molecules is whether LEED will have sufficient sensitivity to the various atomic positions to allow a structural determination. We would like to determine the internal structure of the molecule as well as the molecule's position with respect to other molecules and to atoms in the substrate. We present here model calculations that confirm that surface structure analysis by LEED has enough sensitivity to determine the desired locations of non-hydrogen atoms. It then becomes important to consider the computation effort and find ways to reduce it. We shall test several approximations within the Combined Space Method,[6] which is a natural choice for computing LEED intensities for many adsorbed molecules. Since the computation effort is strongly enhanced by the presence of multiple scattering, the approximations that we test will concentrate on the selective neglect of certain classes of multiple scattering paths. These approximations will be shown to retain in

large part the structural sensitivity of "exact" methods. In particular, approximations based on "near-neighbor multiple scattering" will be introduced in which only the multiple scattering between atoms close to each other is included. Benzene-like C_6 molecules without hydrogen are chosen as a test case since they present many of the features of interest of large molecules.

2. Sensitivity of LEED I-V curves to positional parameters

As surface model for large hydrocarbon molecules we choose a stack of layers, each composed of distinct rings of 6 carbon atoms (hydrogenless benzene molecules). Within a layer, the molecules are arranged basically as shown in Fig.1 with intermolecular distances compatible with touching benzene (C_6H_6) molecules. The identical layers are stacked without lateral shift to maintain the high symmetry of the individual layers. (Benzene does not crystallize in this structure but seems to be able to grow epitaxiallly on substrates in approximately this fashion[7].) The interlayer spacing is chosen to be either 1.5 or 2.5 Å , rather smaller than the distance one would expect from Van der Waals molecular sizes (about 3.4 Å), to allow sizable interlayer effects. This system provides a realistic mix of small and large interatomic distances common in molecular crystals. Compared to the close-packed metals, one notes the small number of nearest neighbors, 2 in this case, and more generally the small number of atoms having the same distance to a given reference atom.

To test the sensitivity of I-V curves to the atomic arrangement, the Combined Space Method[6] (CSM) is used to calculate I-V curves for the model surface, thereby including all relevant multiple scattering. Specifically, Renormalized Forward Scattering (RFS) is used between the layers,[8a] as many layers being included as is necessary for convergence. The multiple

scattering within each layer of 6 atoms per unit cell is included with the Reverse Scattering Perturbation (RSP) method,[8b] which is limited to 8 iteration passes; this limit is usually amply sufficient in typical metal surfaces. Normal incidence of the primary electron beam is chosen in most of our calculations to benefit from symmetry. A spherical carbon atomic potential has been chosen which was previously used by Kesmodel[4] for C_2H_2 and C_2H_4, and angular momenta up to $\ell_{max}=4$ are allowed. A Debye temperature of 973 K and a surface temperature of 300 K are used. The imaginary part of the inner potential V_{oi} is set to 5 eV, an average value often used to represent inelastic effects in metals, semiconductors, and insulators. Typical molecular layers with their fewer collective electronic excitations and relatively small overall electron density may give rise to weaker inelastic effects and thus to smaller values of V_{oi} than metals. However, when electrons in π orbitals such as in the benzene rings are relatively delocalized, inelastic effects may be expected to increase again somewhat.

We shall submit the model surface to three kinds of structural change. Within each change, the lattice constant, i.e. the distance between molecular centers, and the layer spacing remain fixed.

a. The first variation starts with the layer structure of Fig.1 and expands each molecule about its center in equal steps such that each atom moves radially by about 0.18 Å at a time (see ring a in Fig.1). The last step leads to a graphitic (honeycomb) arrangement of C atoms with a reduced unit cell so that 2/3 of the beams are extinguished. At each step a 6-fold rotational symmetry axis and 6 mirror planes are present. Representative I-V curves are shown in Fig.2. Notable is the small effect of the molecular expansion on the specular (00) beam. This results from the fact that all the atomic motions are perpendicular to

the momentum transfer of the specular reflection since this momentum transfer is perpendicular to the surface. The isolated peak at 90 eV for the middle specular curve of Fig.2 most likely stems from a convergence problem; it is a significant feature that will be discussed in Section 4. The non-specular beams are noticeably affected by the structural variation. The effect is similar in magnitude to that of a registry shift of a 1-atom per unit cell overlayer (as in simple atomic adsorption). (There a 0.2 to 0.3 Å shift parallel to the surface is comparable in effect to a 0.1 Å change in layer spacing.) Thus enough sensitivity is present to determine atomic displacements parallel to the surface of the order of 0.2 Å , this value being of course to some extent dependent on the quality of other theoretical parameters such as the atomic scattering parameters.

b. The next geometrical variation of the carbon rings is a rotation of each molecule about its axis of 6-fold symmetry, see ring b of Fig.1. This tests the relative positions of molecules, as opposed to the internal structure of molecules tested above. In Fig.3 are drawn I-V curves calculated for rotations in steps of 7.5°, starting with the geometry of Fig.1 and terminating at a 30° rotation. Now only a 6-fold axis is always present. The specular beam is even less sensitive to this structural variation than to the expansion discussed above. The non-specular beams show varying amounts of sensitivity, but less than is usually experienced in structural determinations of simpler surfaces; peaks shift here by only small amounts, although relative peak heights change markedly. This level of sensitivity is not further reduced if one averages over domains rotated through opposite angles (i.e. through rotations by + α and - α), as one might have to do in the case of layers adsorbed on a

substrate. No increase in sensitivity was found in other tests involving similar rotations. Thus a large off-normal angle of incidence (θ=40°) of the electron beam did not help. Also a buckling of the C_6 rings did not enhance the sensitivity under rotation.

The structural variations discussed above contained no movements perpendicular to the surface, unlike the next case.

c. We now allow the 6-carbon rings to gradually buckle into the "chair" shape that cyclohexane (C_6H_{12}) adopts, i.e. alternate carbon atoms move in opposite directions perpendicular to the plane of the ring, see ring c in Fig.1. Starting with the geometry of Fig.1, the atoms are displaced in steps of 0.1 Å , so that at each step a spacing of 0.2 Å is added between atoms within the same layer (but the average spacing between separate layers is kept constant). Now a 3-fold rotational symmetry exists, together with three mirror planes. Representative I-V curves are shown in Fig.4. This time the specular I-V curve clearly changes appreciably with these atomic displacements parallel to the momentum transfer. In fact, the I-V curves for most beams change substantially, which confirms the long known sensitivity of LEED to structural change perpendicular to the surface. One notices both here and in Figs. 2 and 3 the persistence of some underlying peak structures; these are mostly due to the wave interference between separate layers whose distance remains constant, and are now modulated by the intralayer geometry changes. (We note that in Figs. 2 and 3 an interlayer spacing of 1.5 Å was chosen, while in Fig.4 its value is 2.5 Å to avoid close spacings between atoms in adjoining layers.)

3. Approximations in the multiple scattering formalism

LEED calculations that involve many atoms per unit cell in a layer can rapidly become very cumbersome. We shall explore the effect of approximations in the multiple scattering formalism that reduce the computational effort and we shall assess their usefulness in structural determination.

In the Combined Space Method, one defines atomic layers by requiring that the resulting interlayer spacings (measured between the closest nuclear planes of adjoining layers) be at least about 1 Å , while interplanar spacings within each layer should be less than about 1 Å . This allows the most efficient use of plane waves between layers, spherical waves being used within layers.[6] If a layer has N atoms per unit cell, each of these atoms together with its periodicially equivalent atoms defines a "subplane" of the layer. For example, the layer pictured in Fig.1 has 6 atoms per unit cell and therefore 6 subplanes. One such subplane is emphasized as thick circles in Fig.5 for a similar layer.

The full dynamical calculation first computes the multiple scattering within each isolated subplane i, which involves a matrix inversion (more exactly the solution of a set of linear equations):

$$\tau^i_{LL'} = \left[\left(1 - t^i G^{ii}\right)^{-1}\right]_{LL'} t^i_\ell \qquad (1)$$

Here L=(ℓ,m) and L'=(ℓ ',m'); t^i is the scattering t-matrix of a single atom in subplane i and is obtained directly from phase shifts δ_ℓ through (in atomic units where $\hbar$=e=m=1)

$$t^i_\ell = \frac{1}{2k_o} e^{i\delta_\ell} \sin\delta_\ell \quad , \ell = 0,1,\ldots,\ell_{max}; \; k_o = \sqrt{2(E - V_o - iV_{oi})} \qquad (2)$$

(V_o+iV_{oi} is the complex inner potential). The matrix G^{ii} is a special

case of the Green function G^{ji} that we write as a lattice sum involving arbitrary atoms $\underline{r}_i$ and $\underline{r}_j$ in subplanes i and j, respectively, and all lattice vectors $\underline{P}$ (defining the periodicity)

$$G^{ji}_{LL'} = \sum_{\underline{P}} G_{LL'}(\underline{P} + \underline{r}_j - \underline{r}_i) \qquad (3)$$

(the complete formula is given in Ref.6 and is not needed in the present discussion). The lattice sum is limited in extent by the electron damping represented by V_{oi}. The dimension of the matrices G^{ii} and τ^i is $(\ell_{max}+1)^2$, i.e. the number of spherical waves present for angular momenta up to $\ell = \ell_{max}$.

The next step calculates the multiple scattering beween the subplanes of a layer, given τ^i of Eq.1. In the case of Fig.5, this basically adds to τ^i the multiple scattering between atoms within the individual molecules and between inequivalent atoms in different molecules. One obtains matrices $T^i_{LL'}$, representing all multiple scattering paths within the layer that terminate at subplane i. Using Beeby's formalism[9] these matrices, arranged in vector form, are given by

$$\begin{pmatrix} T^1 \\ T^2 \\ \cdot \\ \cdot \\ T^N \end{pmatrix} = \begin{pmatrix} 1 & -\tau^1 G^{12} & \cdots & -\tau^1 G^{1N} \\ -\tau^2 G^{21} & 1 & \cdots & -\tau^2 G^{2N} \\ \cdot & \cdot & & \cdot \\ \cdot & \cdot & & \cdot \\ -\tau^N G^{N1} & -\tau^N G^{N2} & \cdots & 1 \end{pmatrix}^{-1} \begin{pmatrix} \tau^1 \\ \tau^2 \\ \cdot \\ \cdot \\ \tau^N \end{pmatrix} \qquad (4)$$

and thus involve the inversion of a large matrix of dimension $N(\ell_{max}+1)^2$. When the multiple scattering is not excessively strong, the matrix inversion step can be replaced by a perturbation expansion in terms of the number of backscatterings, called Reverse Scattering Perturbation (RSP).[8b] In the results discussed in this work we have used this expansion. It mainly saves core space rather than computing time in the cases considered

here. However, the approximations that we shall introduce are most effective within the RSP method as they directly reduce the number of terms that are to be included in the calculations. The detailed formalism of RSP is relatively more involved than that of Eq.4 and we therefore prefer for comprehensibility to pursue our discussion in terms of Eq.4 rather than the expansion.

To obtain the layer reflection and transmission coefficients for the scattering of a plane wave $\underline{g}$ to a plane wave $\underline{g}'$, the matrices T^i, which are given in the spherical wave representation in Eq.4, are converted to the plane wave representation through[6]

$$M^{\pm\pm}_{\underline{g}'\underline{g}} = -\frac{16\pi^2 i}{A} \sum_{LL'} \frac{Y_L(\underline{k}^{\pm}_{\underline{g}'}) Y_{L'}^*(\underline{k}^{\pm}_{\underline{g}})}{k^{+}_{\underline{g}'\perp}} \sum_{i=1}^{N} \left[R^{i\pm}_{\underline{g}} (R^{i\pm}_{\underline{g}'})^{-1} T^i_{LL'} \right]. \qquad (5)$$

Here A is the unit cell area, Y_L are spherical harmonics and $\underline{k}^{\pm}_{\underline{g}}$ are the wavevectors for each beam $\underline{g}$, + and - indicating propagation towards, resp. away from the inside of the surface; we also have used the quantities

$$R^{i\pm}_{\underline{g}} = \exp(\pm i\underline{k}^{\pm}_{\underline{g}} \cdot \underline{r}_i). \qquad (6)$$

Before proposing approximations to these formulae, we should discuss how multiple scattering depends on the structure being investigated, specifically in the case of molecules as compared to the more familiar case of metals. The amount of multiple scattering can be small for several reasons. First, the atomic scattering amplitude t^i can be relatively small, as is the case with low atomic number elements, especially H but also C, O and N. Note that these are the most common elements encountered in molecules of practical interest, such as organic molecules. Second, the density of the material can be relatively small and thereby reduce the chance of an electron being elastically scattered within its inelastic

mean free path length. Thus the inelastic effects become relatively large compared to the elastic effects. This holds for alkali metals, condensed inert gases, aluminum, silicon, graphite, and of course for molecular crystals, all of which have densities several times smaller than those of typical transition metals. In the case of molecular crystals, (and for silicon and graphite) one can also think in terms of a reduced number of nearest neighbors, of next nearest neighbors, etc. as is directly apparent in Fig.5; a given atom has a smaller chance of receiving waves scattered from neighboring atoms than in metals or in other dense material. Third, large vibrations reduce the amount of multiple scattering as is described by the Debye-Waller factor which effectively reduces the atomic scattering amplitude.[6,8a] Typical molecules have atomic vibration amplitudes that can be 50-100% larger than for metals at the same temperature. Especially terminal atoms at the end of chains can have large vibration amplitudes. However, in multiple scattering as opposed to single kinematic scattering, the correlations between the motions of neighboring atoms, i.e. their concerted motions, are also important and tend to counteract the effect of the kinematic Debye-Waller factor.[10] Neighboring atoms that do not vibrate strongly with respect to each other may nevertheless undergo large amplitude vibrations together with respect to the surrounding material.

There are factors that can enhance multiple scattering. First, small bond lengths provide a higher chance of second and subsequent elastic scatterings within a given inelastic mean free path length. This is particularly relevant to the common molecules composed of C, N, O, and H, where the nearest-neighbor bond lengths vary beween about 1.0 and 1.5 Å as compared with bond lengths ranging between 2.5 and 3.0 Å in metals. Second, the inelastic mean free path length itself may be larger

than in metals,[11] namely when fewer single electron and collective excitations are available for inelastic interactions. This can happen especially with low-Z substances and with molecules that have few delocalized orbitals.

Our approximate LEED calculations will help us evaluate the strength of multiple scattering in organic layers. We start the detailed description of approximations and their effects by plotting in Fig.6, curves a, "exact" I-V curves for a stack of two layers of the type shown in Fig.5; they are exact in the sense that the RSP and RFS expansions have converged and they are exact within the bounds of the parametrization of atomic scattering amplitude, damping, thermal effects, etc. (The choice of two rather than more layers will be discussed in the next Section.)

Neglect of intra-subplane multiple scattering

Our first approximation consists in removing some multiple scattering between molecules by setting $\tau = t$ (cf. Eqs. 1 and 4). This removes the multiple scattering between periodically equivalent atoms in different molecules; some intermolecular multiple scattering is left, namely that between periodically inequivalent atoms of different molecules, especially between atoms that are close to each other. In so doing we remove relatively unimportant multiple scattering (on account of its relatively long path lengths), the small effect of which is seen in the approximate I-V curves of Fig.6, curves b. The major gain in computation effort results from the skipping of the matrix generation and inversion leading to τ in Eq.1 and the use of a diagonal matrix t instead of the full matrix τ in Eq.4.

Because τ can in fact be blockdiagonalized into two smaller matrices, on which all operations are performed separately, the gain in computation speed is reduced, however.

Nearest-neighbor multiple scattering with variable scattering chain length

The next degree of approximation involves leaving multiple scattering only between nearest neighbors, e.g. between each carbon atom and its two carbon bonding partners. An additional option available within the RSP scheme (but not within the Beeby matrix inversion scheme) is to limit the number of successive nearest-neighbor hops that are allowed, i.e. the permissible length of the chain of nearest-neighbor scatterings, including any looping back to atoms from which scattering has already taken place. We have chosen to allow only chains of length up to 8 (Fig.6, curves c) or up to 1 (Fig.6, curves d), which is simply controlled by the number of passes in the RSP scheme. The nearest-neighbor-only approximation is achieved by setting $\tau = t$ and restricting the sum of Eq.3 to vectors $\underline{P}$ such that $|\underline{P}| < r$, where r is larger than the nearest-neighbor distance but smaller than the next-nearest-neighbor distance, as illustrated by a small limiting circle around one atom in Fig.5. A somewhat larger change is now observed in the I-V curves shown in Fig.6, curves c, compared to when we employed the previous approximation, but the main peaks are not appreciably shifted; only their relative heights are changed. The computational advantage now arises from a much reduced summation in Eq.3, the vanishing of several matrices G^{ji} and the resulting reductions in succeeding operations, in addition to the advantages described in the preceding approximation.

Kinematic approximation

Next we perform a nearly kinematic calculation in which the diffraction

matrix elements for each layer neglect all multiple scattering within the layers. Only the Renormalized Forward Scattering now includes multiple scattering, namely that between the different layers (this is the Quasi-Dynamical method used previously in other, simpler materials[12]). Again, peak positions are not markedly affected, as is seen in Fig.6, curves e, while relative peak heights do change, which may affect the combined shape of overlapping peaks. Computation times of course benefit greatly from the kinematic approximation (we have not determined the time gains as they would only become fully realized under optimal recoding of the computer programs to exploit all the possibilities provided by the approximation).

For comparison, Fig.6, curves f, show I-V curves due to a single layer of 6-carbon rings within the kinematic approximation, rather than for a stack of such layers. The lack of peaks in these curves shows that most of the peaks observed in Fig.6a-c are due to interference between different layers. It is interesting to observe that the 1-layer curves of Fig.6f, which contain the kinematic structure factor of the rings, are almost featureless; the structure factor of the C_6 rings has surprisingly little structure as a function of energy and angle, at least at our low energies.

The peaks in the I-V curves for the stack of layers are influenced by the transmission and reflection coefficients of all layers, as has been discussed elsewhere.[6] The fact that these peaks have hardly shifted in energy under the various approximations shows that the layer diffraction matrices have not suffered substantially in those approximations, especially as far as their phases are concerned, which are the main factors affecting peak positions.[6] We may thus conclude that the sensitivities of I-V

curves exhibited in Section 2 will also carry over to the approximated I-V curves, which is confirmed by corresponding calculations. Together with the fact that peak positions are mainly sensitive to atomic positions (rather than non-structural parameters), this is of great importance in structural determination since it allows one to perform a structural determination with its possibly long geometrical search by using economical and efficient approximations such as those discussed here. Clearly the accuracy of a structural determination will decrease as the approximation becomes more severe. Nevertheless, an application of this approach to to Rh(111)+(2x2)C_2H_3, with the kinematic approximation in the overlayer and neglecting the H atoms, produced the correct structural result within about 0.1 Å , using an R-factor search with actual experimental data, as illustrated in Fig.7c.(for more details, see Ref.5). Thus a stage-wise determination is indicated where in the first stage a severe but time efficient approximation can identify a few promising structures among a long list of possibilities. Then a second stage can further discriminate between the few promising structures and/or refine them with a less severe approximation. A series of such stages can be imagined.

A note about computational aspects will conclude this Section. In the kinematic limit, Eq.5 only changes in the sense that $T^i_{LL'} = t^i_\ell \delta_{\ell\ell'} \delta_{mm'}$ becomes diagonal, with trivial summations over ℓ ' and m' to get

$$M^{\pm\pm}_{\underline{g}'\underline{g}} = -\frac{4\pi i}{A} \sum_\ell \frac{2\ell+1}{k^+_{\underline{g}'\perp}} P_\ell(\cos\theta^{\pm\pm}_{\underline{g}'\underline{g}}) \sum_{i=1}^{N} \left[R^{i\pm}_{\underline{g}} \left(R^{i\pm}_{\underline{g}'}\right)^{-1} t^i_\ell \right], \qquad (7)$$

where θ is the complex scattering angle between beams $\underline{g}^+$ and $\underline{g}^+$.

This expression may at first sight seem computationally more efficient than Eq.5 with a kinematic $T^i_{LL'}$. However, one must also consider the

effects of repeated calculations with variable atomic positions and of available symmetries that can be put to advantage. With variable atomic positions one should store the constant quantities $P_\ell(\cos\theta^{\pm+}_{\underline{g}'\underline{g}})$ for all $\ell, \underline{g}^{\pm'}$ and $\underline{g}^{+}$

or at least $\cos\theta^{\pm+}_{\underline{g}'\underline{g}}$ for all $\underline{g}^{\pm'}$ and $\underline{g}^{+}$. When symmetries between beams are taken advantage of, the number of such quantities is not simply reduced to that corresponding to non-degenerate beams $\underline{g}$. This is because $\cos\theta^{\pm\pm}_{\underline{g}''\underline{g}}$ is not simply related $\cos\theta^{\pm\pm}_{\underline{g}'\underline{g}}$ even when $\underline{g}''$ and $\underline{g}'$ are symmetry-related, unlike the case of $Y_L(\underline{k}^{\pm}_{\underline{g}''})$ and $Y_L(\underline{k}^{\pm}_{\underline{g}'})$, (see Ref.6). So Eq.5 retains some advantages, despite the extra summation over m and the correspondingly large number of L-values, namely $(\ell_{max}+1)^2$, since in the case of Eq.5 only $Y_L(\underline{k}^{+}_{\underline{g}})$ need be stored for all L and $\underline{g}$. Thus whether Eq.5 or Eq.7 is most efficient depends on the relative numbers of spherical waves and beams, as well as on the kind of symmetry present, the number of geometry variations planned, and the relative cost of storage and numerical operations.

4. Convergence questions

Figures 2-4 include several cases of poor convergence that are identifiable through the appearance of unusually sharp peaks in the I-V curves, namely around 85 eV in several beams. Such convergence problems are known to occur with perturbation methods in LEED in cases of strong multiple scattering, in the present case presumably between neighboring carbon atoms, whose distance is of the order of 1.45 Å . Since we have used realistic physical parameters in our model calculations (in particular for the mean free path and the vibration amplitudes), this multiple scattering

should be present in real systems as well. Thus although we are dealing with a low Z element and with few nearest neighbors, the small bond lengths allow considerable multiple scattering to build up to a point comparable with that in strongly scattering metals.

As we have seen, the neglect of multiple scattering, even in the kinematic limit within each layer, does not shift existing peak positions in I-V curves enough to particularly impair structural determination, especially if peak heights are disregarded. The main risk is that spurious peaks develop that could influence a structural determination. Such spurious peaks are due to the lack of current conservation that approximations entail: artificial excesses of electron current can be multiplied in the multiple scattering process. One example of non-convergence occurred around 85 eV when an infinity of 6-carbon-ring layers (rather than a pair of such layers) were stacked together and RFS was applied to that semi-infinite stack, i.e. the spurious peaks of Fig.6 blew up. This led to our choice of only two layers in the case of approximations. In cases like this one, a better approach could be to restrict the multiple scattering between the layers to avoid the buildup of errors; this can be achieved, for example, by limiting the number of passes allowed in RFS, or by combining a few layers into one single layer within which the chosen approximations are applied.

One can sometimes visually detect and then ignore spurious peaks, but an R-factor analysis would blindly include such peaks and may be led astray in its structual predictions (however an R-factor sensitive to peak positions rather than peak heights and shapes should still be effective). It may pay off in that case to artificially reduce the

multiple scattering in order to avoid such spurious peaks. This may be achieved in the calculation by shortening the mean free path length (which is just another way of shortening the scattering paths) and/or by increasing the atomic vibration amplitudes to reduce the atomic scattering factors. It is well known that such manipulation does not in first approximation shift peak positions and should therefore not markedly impair the capability of structural determination.

In the context of molecular layers adsorbed on metal surfaces, it is generally recommendable to make less severe approximations within the metal than within the molecular layers, because of the usually greater predominance of multiple scattering in most metals. This can easily be implemented in the traditional layer approach by employing different levels of approximation within different layers and combining the layers with any of the known methods (RFS, transfer matrix method, layer doubling, Bloch waves, etc.).

5. The near-neighbor multiple scattering model

Let us examine the nature of some of our approximations in a different light. If we take the approximation which allows only single-length scattering paths and scatterings between nearest neighbors, we see that we have in effect allowed multiple scattering only within the small cluster composed of any given atom and its nearest neighbors. This cluster idea also appears in a different way as follows. It is apparent from Eq.5 which, in the kinematic limit, would have the factors $t_\ell^i \delta_{\ell\ell'} \delta_{mm'}$ replacing $T_{LL'}$, that the exact layer diffaction properties are in fact calculated as a kinematical lattice sum over each of the total scattered waves leaving each atom of the layer. It is thus as if each atomic scattering factor t_ℓ^i of Eq.2 that appears in a kinematical formula had

simply been replaced by a more complex scattering factor that includes the multiple scattering effect of the lattice surrounding that atom, i.e. of a cluster of not too distant atoms.

It is then natural to think of the approximations mentioned above as consisting of the replacement of each atom by a "cluster-embedded" atom that includes the multiple scattering effect of its nearest neighbors within the cluster. This near-neighbor multiple scattering model is formally equivalent to that described in the last sections (based on layers with subplanes) but provides two main advantages. First, it is the basis of a new class of approximations that is characterized by the use of embedding clusters of any suitable size and shape;[13] if desired, various limitations on the multiple scattering within the cluster can also be included. Second, the near-neighbor multiple scattering model permits the storage of the cluster scattering properties for multiple use after a single calculation, because such clusters can be rotated easily in space, which is not readily done in the layer-with-subplane approach. This advantage can be derived from Pendry's formalism for dealing with the exact scattering from finite clusters of atoms[1a,14], as will be shown below.

The effect of the near-neighbor multiple scattering approximations on I-V curves is similar to that shown in Section 3 for the various approximations discussed there, since these approximations partly overlap. Our experience with those approximations thus allows us to state that the near-neighbor multiple scattering approximations also provide a useful basis for structural analysis of surfaces.

To formalize the above considerations, let us define the t-matrix $T^{ii}_{LL'}$ to represent all those multiple scattering paths within a certain

cluster c of atoms that start at atom j and terminate at atom i, both atoms j and i belonging to that cluster c. Again, approximations may involve neglecting some of these multiple scattering paths within the cluster. $T^{ij}_{LL'}$ represents the amplitude of a scattered spherical wave L=(ℓ m) due to an incident spherical wave L'=(ℓ 'm'), both waves being centered on the same artibrary point, e.g. on atom i. This is the same quantity defined by Pendry in Eq.27 of Ref. 1a, if one omits his summation over j and k, which stand for our i and j. An effective atom i is then represented by replacing its individual t-matrix t^i by the t-matrix $T^{i,c} = \sum_j T^{ij}$, where j ranges over all atoms in the cluster c, including i itself. $T^{i,c}$ thus includes all scattering paths within the cluster that terminate at atom i. In the 6-carbon ring case, each of the six C-C-C triplets gives rise to a t-matrix $T^{i,c}$ representing each of the six central atoms of the C-C-C fragments. This t-matrix $T^{i,c}$ then takes the place of T^i in Eq.5.

Two distinct clusters around atom i can be added, with some precaution to avoid double counting of paths. Thus clusters c_1 and c_2 with the common atom i can be added as follows: $T^{i,c_1+c_2} = T^{i,c_1} + T^{i,c_2} - t^i$, where the single scattering by atom i itself is subtracted to avoid double inclusion. Note that T^{i,c_1+c_2} is not equal to the exact $T^{i,c}$ matrix of the complete cluster $c=c_1+c_2$, because some paths have been left out, namely those that directly connect any atom other than i in cluster c_1 with any atom other than i in cluster c_2. In the carbon ring example, c_1 could be a cluster composed of one carbon atom and one of its neighbors, while c_2 would be the cluster composed of the same carbon atom and its other neighbor.

As pointed out by Pendry[1a,14] any of the t-matrices used above can be changed in accordance with a rotation of the cluster, through the use

of rotation matrices[15] $R_{LL'}$ that operate in general on a matrix T as $R^{-1}TR$ (the inverse R^{-1} is equal to the transpose of R). Although all these matrices have the potentially large dimension $(\ell_{max}+1)^2$, making matrix multiplications time consuming, one in fact only needs to multiply expressions such as $R^{-1}TR$ by a vector, which contains the $\underline{g}$-dependent factor of Eq .5, i.e. basically spherical harmonics used to transform from the spherical wave representation to the plane wave representation.[6] Therefore, no matrix-matrix multiplication but only the much more economical matrix-vector multiplication is required. In addition, the possibility of rotations allows one also to permanently store the t-matrices for elementary clusters that are often encountered, in order to avoid having to recompute them each time (these matrices should be stored at each energy point, since they are energy-dependent).

6. Summary

We have explored the use of LEED in the structural determination of molecular layers with adsorption on substrates in mind. It has been shown that sufficient sensitivity to positional parameters is present in I-V curves to warrant the continued use of LEED in such cases. In view of the cost of full dynamical calculations in complex systems, a number of appoximations are proposed and several of them tested in a realistic case of layers composed of 6-carbon rings. It appears that the main features of I-V curves needed in surface crystallography, the peak positions, are not strongly affected by those approximations; therefore, these approximations become valuable in reducing the cost of a structural search. However, a negative side effect, the appearance of spurious multiple scattering peaks in I-V curves, is pointed out and cures are discussed.

A new class of approximations using only near-neighbor multiple scattering is introduced which allows multiple use, through permanent storage and spatial rotations, of the scattering properties of small elementary clusters of atoms. It should be particularly helpful in structural searches that require a reliability better than that provided by kinematic approximations.

Acknowledgement

This work was supported by the Director, Office of Energy Research, Office of Basic Energy Sciences, Materials Sciences Division of the U.S. Department of Energy under Contract W-7405-ENG-48.

References

1a. S. Andersson and J.B. Pendry, Phys. Rev. Lett. 43, 363 (1979); J. Phys. C13, 3547 (1980).

1b. K. Müller, E. Lang, P. Heilmann, and K. Heinz, to be published.

1c. M. Passler, A. Ignatiev, F. Jona, D.W.Jepsen, and P.M. Marcus. Phys. Rev. Lett. 43, 360 (1979).

1d. S.Y. Tong, A. Maldonado, C.H Li and M.A. Van Hove, Surf. Sci. 94, 73(1980).

2. R.J. Behm, K. Christmann, G. Ertl, M.A. Van Hove, P.A. Thiel, and W.H. Weinberg, Surf. Sci. 88, L59 (1979).

3. R.J. Koestner, M.A. Van Hove, and G.A. Somorjai, Surf. Sci. xxx, xxx (1981).

4. L.L. Kesmodel, L.H. Dubois, and G.A. Somorjai, J.Chem. Phys. 70, 2180 (1979).

5. M.A. Van Hove, R.J. Koestner, and G.A. Somorjai, to be published.

6. S.Y. Tong and M.A. Van Hove, Phys. Rev. B16, 1459 (1977); M.A. Van Hove and S.Y. Tong, Surface Crystallography by LEED, Springer (Heidelberg), 1979.

7a. P.C. Stair and G.A. Somorjai, J. Chem. Phys. 67, 4361 (1977).
7b. S. Lehwald, H. Ibach, and J.E. Demuth, Surf. Sci. 78, 577 (1978).

8a. J.B. Pendry, Low Energy Electron Diffraction, Academic (London) 1974.
8b R.S. Zimmer and B.W. Holland, J. Phys. C8, 2395 (1975).

9. J.L. Beeby, J. Phys. C1, 82 (1968)

10. This was investigated in the context of EXAFS in J.J. Rehr, to be published _____; see also Ref. 8a.

11. Experimental values in molecular crystals are rare and ambiguous, see C.R. Brundle, H. Hopster, andJ.D. Swalen, J. Chem. Phys. 70, 5190 (1979).

12. S.Y. Tong, M.A. Van Hove, and B.J. Mrstik, Proc 7th IVC and 3rd ICSS, (Vienna), 1977.

13. This approach has similarities with a formalism developed for disordered surfaces, in which various clusters are averaged together, see H. Jagodzinski, W. Moritz, and D. Wolf, Surf. Sci. 77, 233 and 249 (1978).

14. J.B. Pendry, Proc. Conf. on Determination of Surface Structure by LEED, Plenum (New York) 1981.

15. J.C. Slater, Quantum Theory of Atomic Structure, McGraw Hill (New York), 1960.

Figure Captions

Fig. 1 Atomic structure of one layer of 6-carbon rings. Rings a, b, and c illustrate molecular expansion, rotation, and buckling, as used in the test calculations (+ and - signs refer to positions above and below the molecular plane).

Fig. 2 A selection of theoretical I-V curves for a surface composed of layers of 6-carbon rings, expanding as illustrated in Fig.1a. In each panel, corresponding to separate diffracted beams, curves for increasing expansion are drawn above each other with shifted baselines.

Fig. 3 As Fig.2 for 6-carbon rings, rotating as illustrated in Fig.1b. Curves for increasing rotation are shifted upward.

Fig. 4 As Fig. 2 for 6-carbon rings, buckling as illustrated in Fig. 1c. Curves for increasing buckling are shifted upwards.

Fig. 5 Atomic structure of one layer of 6-carbon rings, with one subplane of atoms emphasized as thick-line circles. A small circle for lattice summation cutoff around one atom is included.

Fig. 6 Theoretical I-V curves for a surface composed of layers of 6-carbon rings (cf. Fig.5): (0,0) and (2,0) beams at normal incidence. The same intensity scale is used for all curves, which are shifted upward for clarity.

a. "exact" calculation;
b. τ = t approximation; no intra-subplane multiple scattering;
c. intralayer multiple scattering between nearest neighbors only in chains up to 8 long;
d. as c. with chains up to length 1;
e. no intralayer multiple scattering (Quasi-Dynamical approximation);
f. kinematic approximation for one isolated layer.

Fig.7 Contour plots of R-factors for the comparison of experimental and theoretical LEED I-V curves for Rh(111)+(2x2) C_2H_3 (ethylidyne with C-C axis perpendicular to surface in hcp-type hollow site; hydrogen ignored in theory). The Rh-C and C-C layer spacings are varied. Panel a uses "exact" (i.e. converged) calculations, while panel b uses the kinematical approximation in the double carbon layer. The plotted R-factor is an average over five different established R-factor definitions, cf. Ref. 5. Contour levels are separated by 0.025.

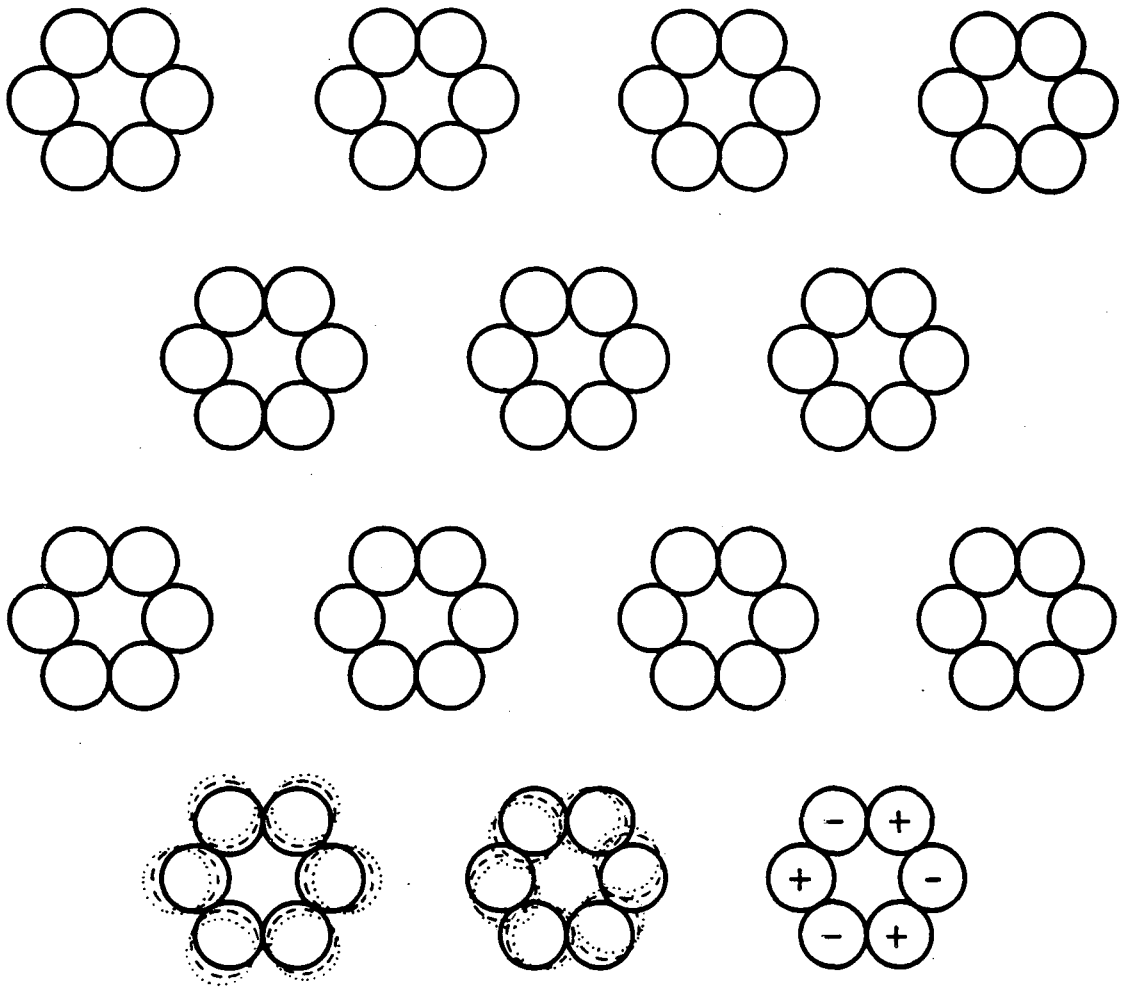

Fig.1

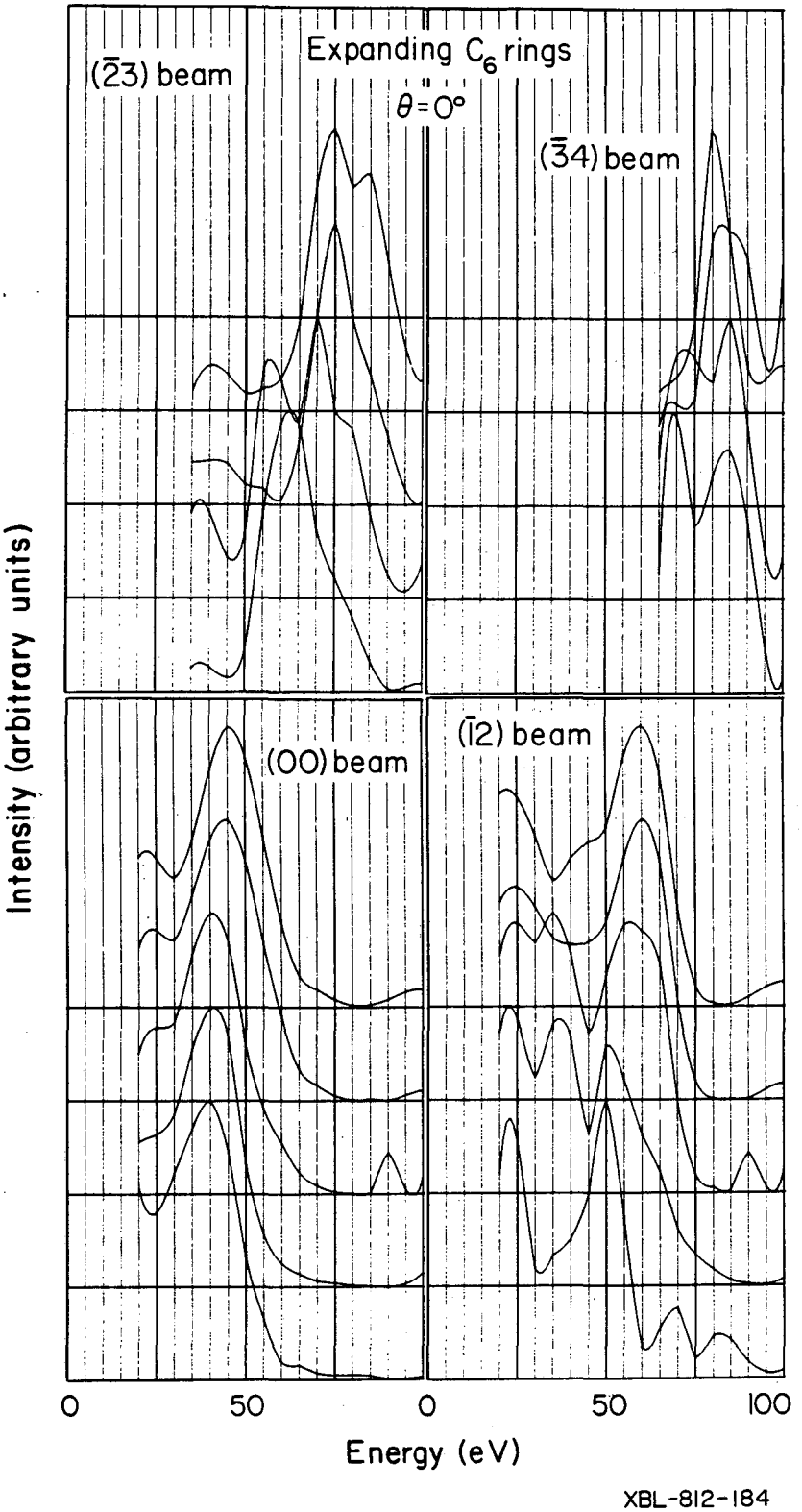
Expanding C_6 rings
$\theta = 0°$
$(\bar{2}3)$ beam
$(\bar{3}4)$ beam
(00) beam
$(\bar{1}2)$ beam
Intensity (arbitrary units)
0
50
0
50
100
Energy (eV)
XBL-812-184

Fig.2

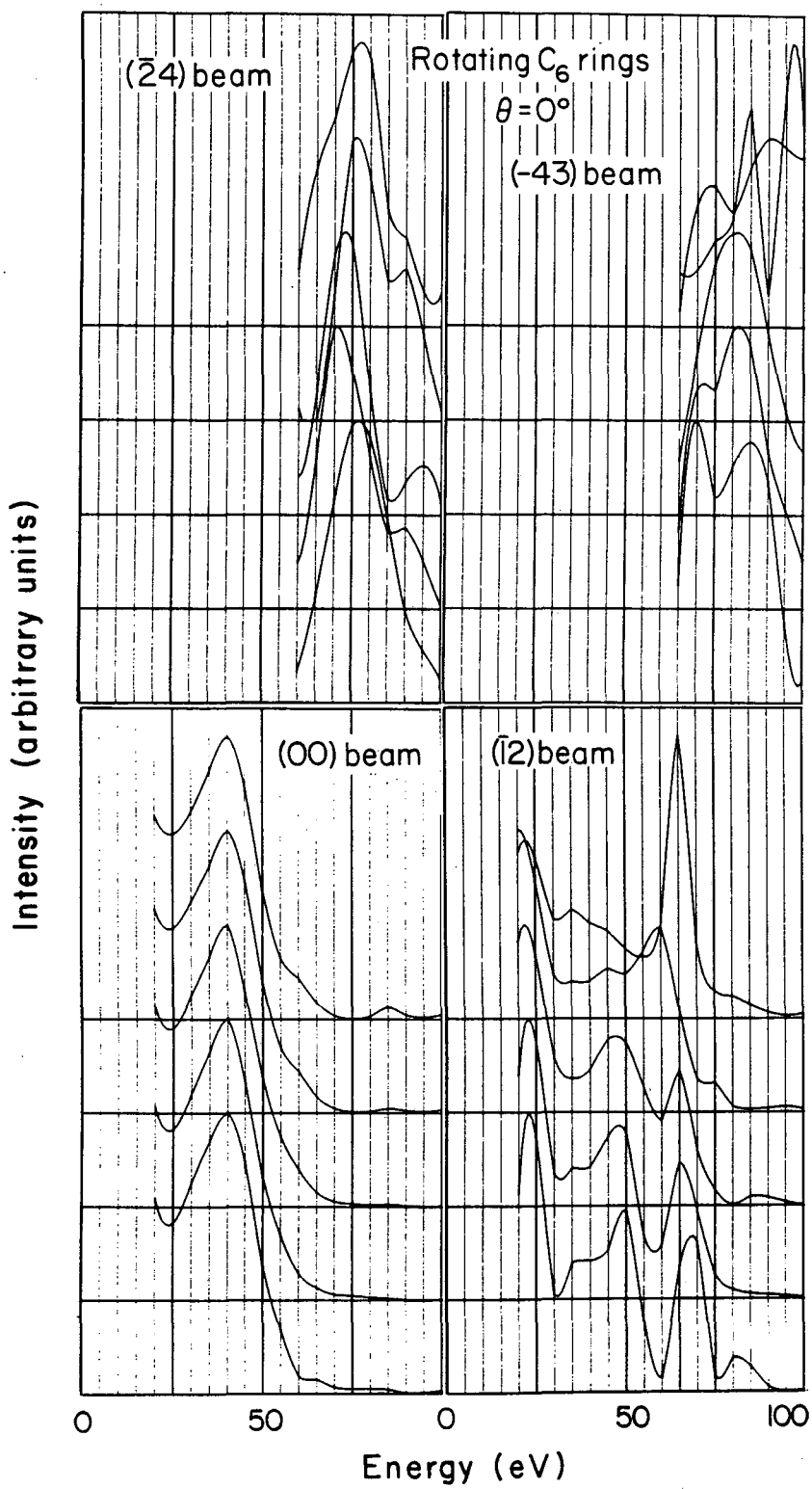
(2̄4) beam
Rotating C_6 rings
$\theta = 0°$
(-43) beam
(00) beam
(1̄2) beam
Intensity (arbitrary units)
0
50
0
50
100
Energy (eV)
XBL-812-182

Fig.3

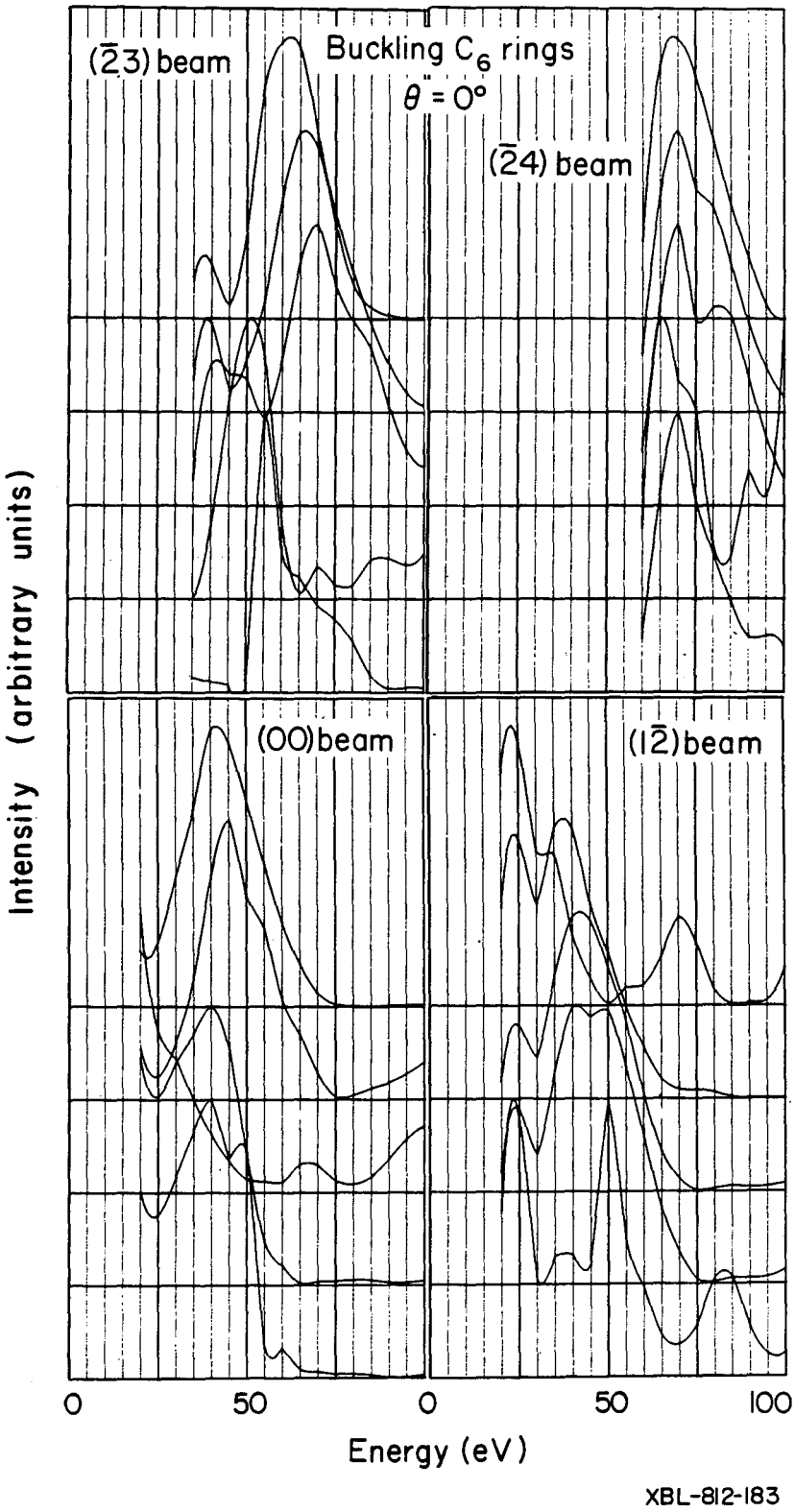
(2̄3) beam
Buckling C_6 rings
$\theta = 0°$
(2̄4) beam
(00) beam
(12̄) beam
Intensity (arbitrary units)
0
50
0
50
100
Energy (eV)
XBL-812-183

Fig.4

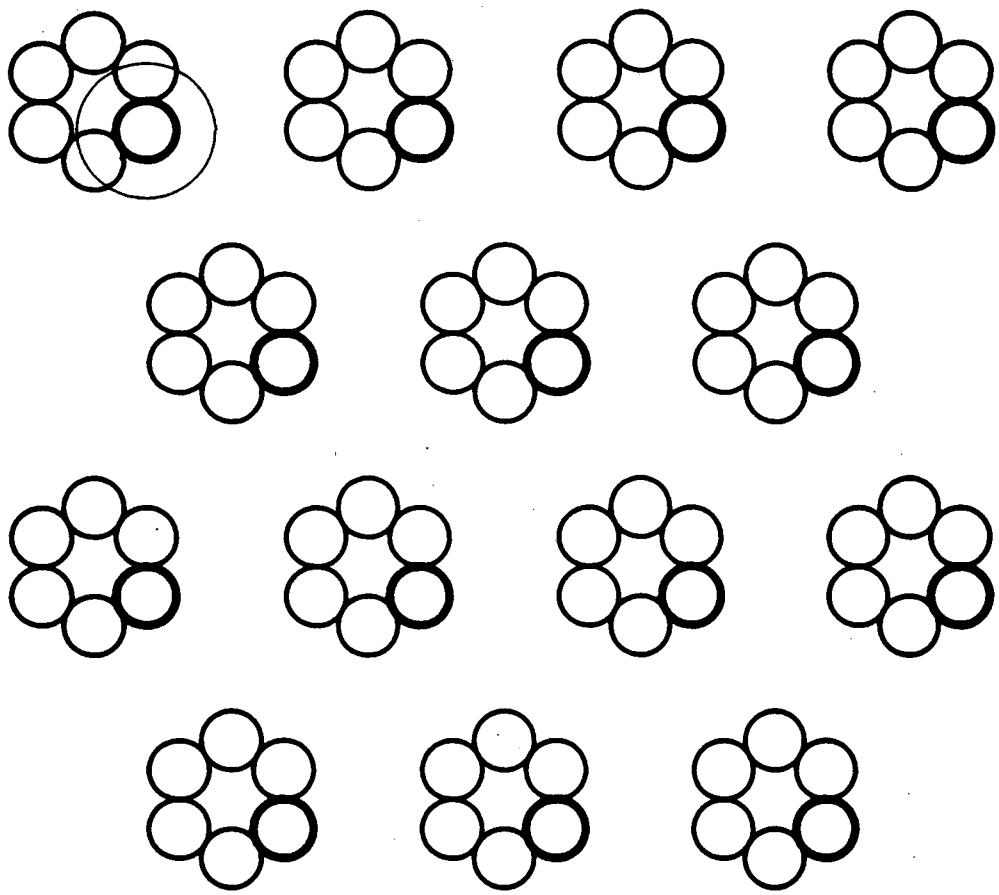

XBL-812-178

Fig.5

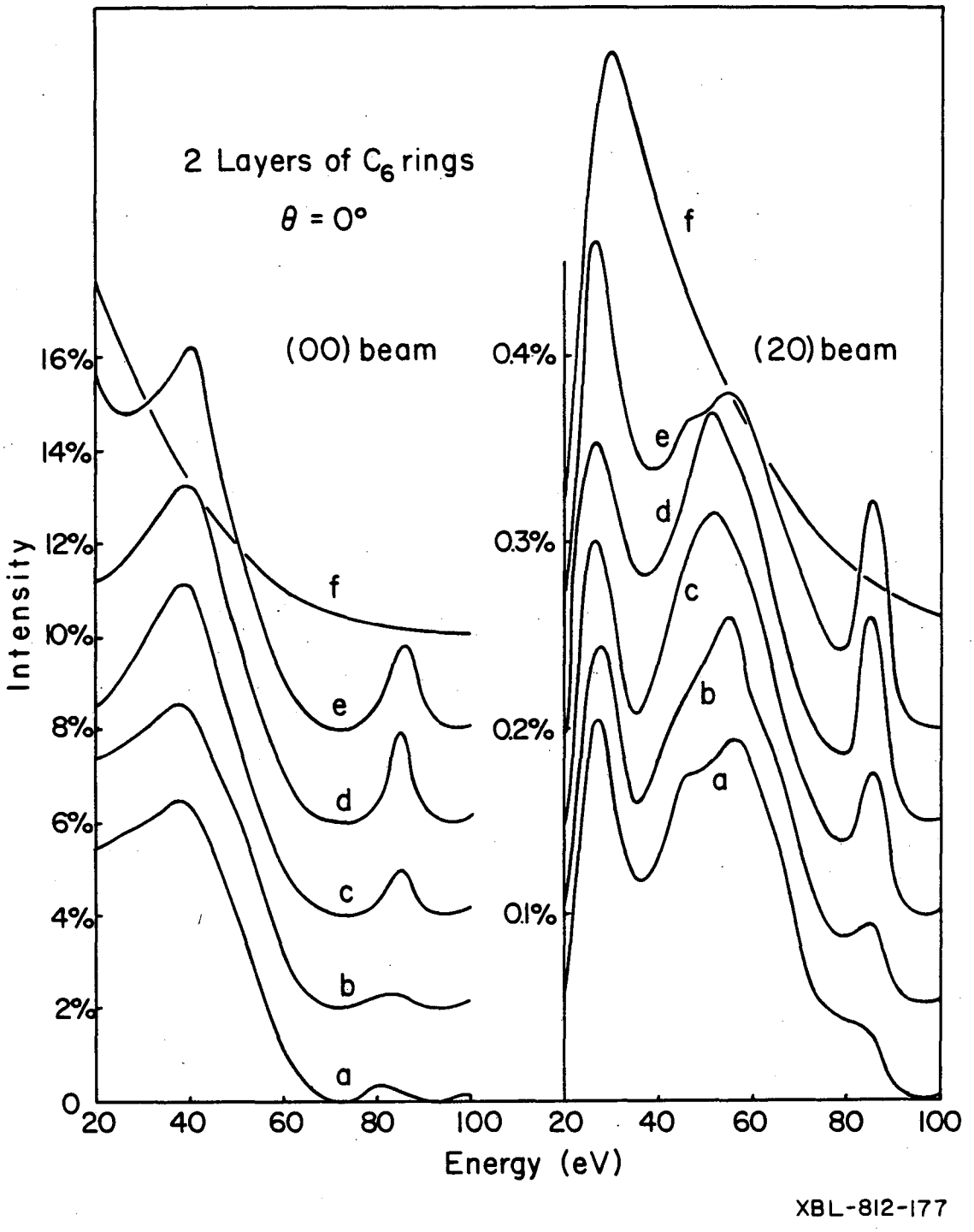
2 Layers of C_6 rings
$\theta = 0°$
(00) beam
(20) beam
Intensity
16%
14%
12%
10%
8%
6%
4%
2%
0
0.4%
0.3%
0.2%
0.1%
a
b
c
d
e
f
20
40
60
80
100
Energy (eV)
XBL-812-177

Fig.6

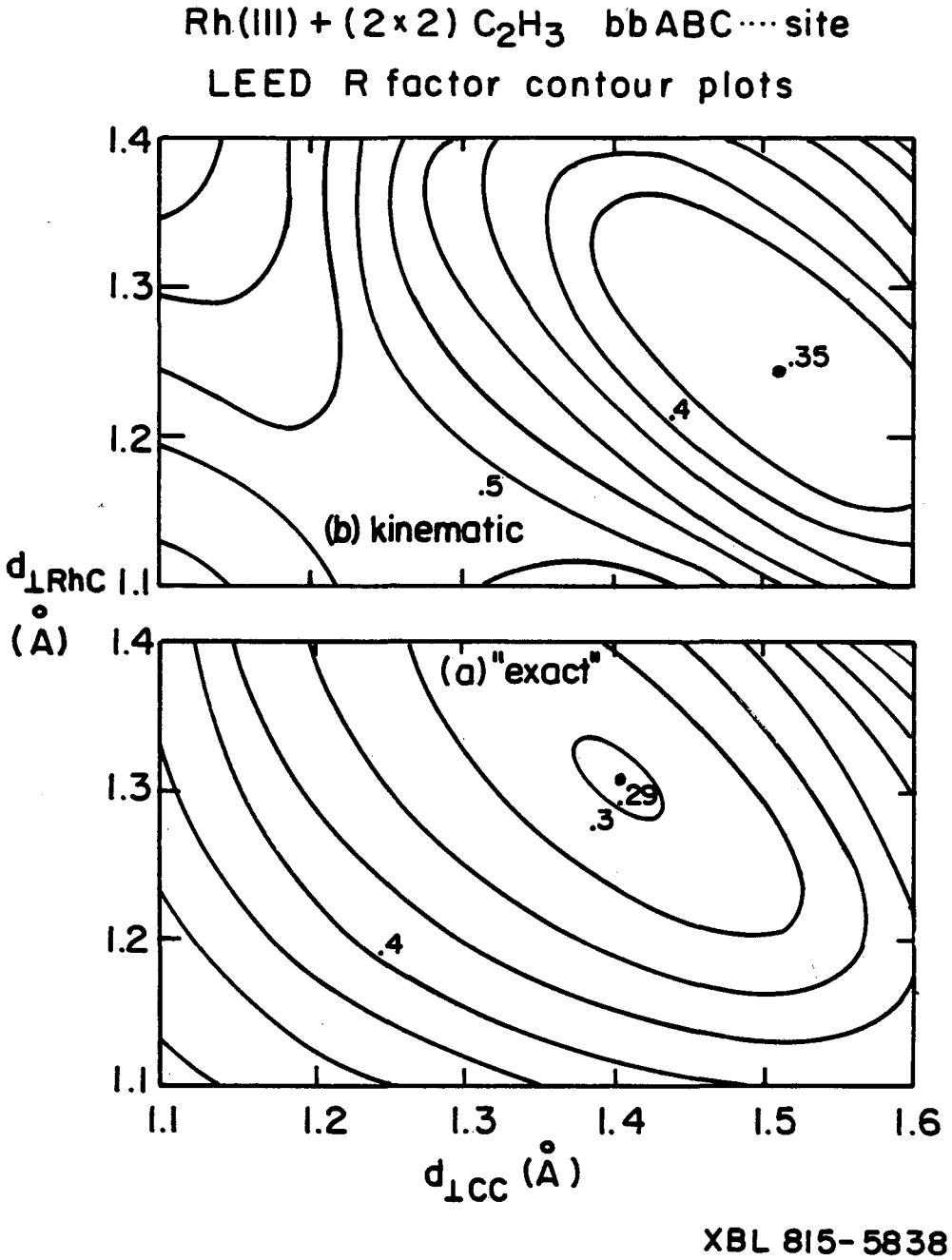
Rh(III) + (2×2) C_2H_3 bbABC···· site
LEED R factor contour plots
(b) kinematic
.35
.4
.5
(a) "exact"
.29
.3
.4
$d_{\perp RhC}$ (Å)
$d_{\perp CC}$ (Å)
1.1
1.2
1.3
1.4
1.5
1.6
XBL 815-5838

Fig.7

TECHNICAL INFORMATION DEPARTMENT
LAWRENCE BERKELEY LABORATORY
UNIVERSITY OF CALIFORNIA
BERKELEY, CALIFORNIA 94720